

# IMPROVING OCEANIC OVERFLOW REPRESENTATION IN CLIMATE MODELS

The Gravity Current Entrainment Climate Process Team

BY SONYA LEGG, BRUCE BRIEGLEB, YEON CHANG, ERIC P. CHASSIGNET, GOKHAN DANABASOGLU, TAL EZER, ARNOLD L. GORDON, STEPHEN GRIFFIES, ROBERT HALLBERG, LAURA JACKSON, WILLIAM LARGE, TAMAY M. ÖZGÖKMEN, HARTMUT PETERS, JIM PRICE, ULRIKE RIEMENSCHNEIDER, WANLI WU, XIAOBIAO XU, AND JIAYAN YANG

Collaboration between observationalists, theoreticians, and process and climate modelers leads to new understanding of oceanic overflows and hence to improved representation in ocean climate models.

The Gravity Current Entrainment Climate Process Team (CPT) was established by the U.S. Climate Variability and Predictability (CLIVAR) Program to encourage the translation of new understanding from observations and process models into new parameterizations and hence improve the representation of oceanic overflows in climate models. Global coupled ocean–atmosphere

models are increasingly used for climate predictions and projections of future climate change (Solomon et al. 2007). The credibility of these models is limited by their ability to represent climatologically important processes, which occur on scales smaller than the climate model grid scale (currently typically 100 km), such as the overflows shown in Fig. 1. These overflows, or dense gravity currents, result when dense water formed behind confining topographic barriers, or on a continental shelf, escapes into the deep ocean over a sloped sea floor. Important examples of the former are the overflows of dense water from the Nordic seas of the northern North Atlantic (Girton and Sanford 2003; Mauritzen et al. 2005) and ►

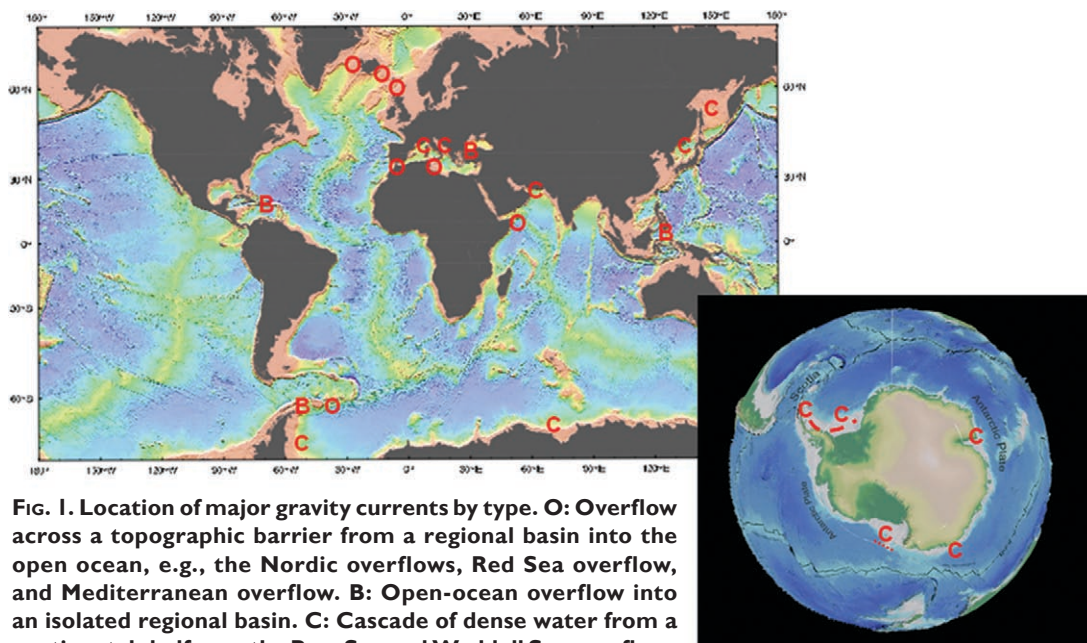


**FIG. 1.** Location of major gravity currents by type. **O:** Overflow across a topographic barrier from a regional basin into the open ocean, e.g., the Nordic overflows, Red Sea overflow, and Mediterranean overflow. **B:** Open-ocean overflow into an isolated regional basin. **C:** Cascade of dense water from a continental shelf, e.g., the Ross Sea and Weddell Sea overflows (see Table 1 for further information). Not shown are numerous overflows across multiple sills of the midocean ridge system, within the series of basins of the western South Pacific; and the cascades of shelf water over the slope of the Arctic Sea. Bathymetry map from Smith and Sandwell (1997).

from the subtropical Mediterranean (Price et al. 1993) and Red Seas (Peters et al. 2005). The continental margin prime example occurs around Antarctica, notably in the Weddell (Foldvik et al. 2004) and Ross Seas (Gordon et al. 2004). Because much of the deep-ocean water masses are derived from the Nordic and Antarctic overflows, the overflow density and transport likely influence the thermohaline circulation.

As dense water passes from its formation site into the open ocean through an overflow, it undergoes mixing with overlying water, determining the eventual properties and volume of the resultant deep-water mass. Credible climate projections require that these overflow processes are represented in ways that reproduce both the modern overflow-derived plumes and any known variations in response to changes in the ambient ocean state. Models without accurate overflow representation may have deep-water formation sites in the wrong locations (i.e., dominated by open-ocean convection in the Irminger and Labrador Seas; Kösters et al. 2005) and incorrect meridional overturning circulation (MOC) vertical structure and heat transport distribution. However, because these processes occur below the grid scale of our highest-resolution global ocean models (or even regional models), realistic representation of overflows poses a considerable challenge for numerical simulation.

Overflows not only influence the deeper water masses (Dickson and Brown 1994), but they may also affect the surface layer temperature and oceanic

heat flux through dynamical coupling with the overlying upper ocean. Localized overflow processes, such as a change in the thickness of the overflow layer or dissipation, can influence the basin-scale circulation and transport (Yang and Price 2007). The entrainment and eddying processes associated with overflows (Kida et al. 2007) can lead to upper-ocean responses in the form of cross-basin beta plumes. Model simulations of thermohaline changes—for example, those induced by large freshwater fluxes in the North Atlantic (Stouffer et al. 2006)—may not be reliable without proper influence of overflows on these processes (as well as improvements in boundary current representation). One goal of our collaboration is to assess the climate effects of new representations of overflows implemented in ocean models.

### **THE CLIMATE PROCESS TEAM: A BRIDGE BETWEEN FIELD OBSERVATIONS, PROCESS MODELING, AND CLIMATE MODEL DEVELOPMENT.**

Field, laboratory, and theoretical process studies of overflows have increased our understanding of overflow processes. However, to translate this detailed understanding into improvements in climate models requires close collaboration with climate model developers. The CPT framework is an attempt to bridge the communication gap between those researchers studying a particular process and the climate model developers—a gap exacerbated by the geographical separation between ocean-going oceanographers and climate modeling centers. Our particular CPT, focused on improving the representation of overflows, is composed of observationalists involved in recent field programs; process study modelers carrying out idealized simulations; and developers of ocean general circulation models used in coupled climate simulations.

Because there are many different aspects to both the physics and simulation of overflows, we do not attempt to describe all of our work and important results in this short article. Instead, we give a brief overview of the different components of our project and then describe two specific examples in more detail: first, new developments in the parameterization of shear-driven mixing in overflows; and second, a case study of the Mediterranean overflow and improvements in its simulation and/or representation in several different models, including regional ocean models, global ocean models, and coupled models. During the course of this collaboration, we have examined several other processes and implemented representations for several other overflows; refer to the reference list for details.

**AFFILIATIONS:** LEGG, EZER,\* AND JACKSON—Princeton University, Princeton, New Jersey; BRIEGLB, DANABASOGLU, LARGE, AND WU—National Center for Atmospheric Research, Boulder, Colorado; CHANG, ÖZGÖKMEN, PETERS, AND XU—University of Miami, Miami, Florida; CHASSIGNET—The Florida State University, Tallahassee Florida; GORDON—Lamont-Doherty Earth Observatory, Columbia University, New York, New York; GRIFFIES AND HALLBERG—NOAA/Geophysical Fluid Dynamics Laboratory, Princeton, New Jersey; PRICE, RIEMENSCHNEIDER, AND YANG—Woods Hole Oceanographic Institution, Woods Hole, Massachusetts

\***ADDITIONAL AFFILIATION:** Old Dominion University, Norfolk, Virginia

**CORRESPONDING AUTHOR:** Sonya Legg, NOAA/GFDL, Princeton University Forrestal Campus, 201 Forrestal Drive, Princeton, NJ 08540  
E-mail: [sonya.legg@noaa.gov](mailto:sonya.legg@noaa.gov)

*The abstract for this article can be found in this issue, following the table of contents.*

DOI:10.1175/2008BAMS2667.1

In final form 22 August 2008  
©2009 American Meteorological Society

A prerequisite of any new parameterization is that it should accurately reproduce the most important features of the observations. Hence, an important task of the CPT has been to consolidate the existing observations of gravity currents (the CPT did not fund any new observations) into a comparative table of observations (shown in abbreviated form as Table 1). The overflows shown here are those that have been

reasonably well sampled and have produced important water masses. The table gives a series of metrics that define the gravity currents, and it presents characteristic values of these metrics, so that the various gravity currents may be easily compared. We find that there are many similarities—for example, the approximate doubling in transport and the occurrence of a region of near-critical Froude number—which

**TABLE 1. The Table of Observations shows comparison of key parameters in different overflows. The source and product water properties serve as a reference against which to evaluate OGCMs. The parameters at the bottom of the table show that while rotation has varying degrees of influence, in all the overflows the Froude number can exceed 1, in regions associated with entrainment. The data are taken from the field campaigns described in the following publications: Faroe Bank: Mauritzen et al. (2005); Denmark Straits: Girton and Sanford (2003); Ross Sea: Gordon et al. (2004); Weddell Sea: Foldvik et al. (2004); Red Sea: Peters et al. (2005); and Mediterranean Sea: Price et al. (1993).**

	Faroe Bank	Denmark Strait	Ross Sea	Weddell Sea	Red Sea	Mediterranean Sea
<b>Source water</b>						
potential temperature °C	0	0.25	-1.9	-1.9	22.8	14.0
salinity	34.92	34.81	34.8	34.67	39.8	38.4
$\sigma_0$	28.07	27.94	27.9	27.8	27.7	28.95
sill depth (m)	800	500	600	500	200	300
<b>Product water</b>						
potential temperature °C	3.3	2.1	-1.0	-1.0	21.7	11.8
salinity	35.1	34.84	34.72	34.67	39.2	36.4
$\sigma_0$	27.9	27.85	27.85	27.75	27.48	27.6
depth (m)	3,000	1,600	>3,000	2,000	750	850
<b>Transport (Sv)</b>						
source	1.8	2.9	0.6	1.0	0.3	0.8
product	3.3	5.2	2	5	0.55	2.3
<b>Velocity <math>U</math> (m s<sup>-1</sup>)</b>						
source	1	0.7	1	1	0.55	1
product	0.5	0.4	0.5	0.4	small	1
<b>Thickness <math>H</math> (m)</b>						
source	200	200	150	100	100	200
product	150	200	250	300	140	200
Transit time source to product (days)	3–5	4–7	1	1	3.5	3–5
Tidal current (m s <sup>-1</sup> )	0.2	0.1	0.3	0.2	0.8	0.1
$g' = g\Delta\rho/\rho_0$		$2 \times 10^{-3}$	$2 \times 10^{-3}$	$2 \times 10^{-3}$	$1.4 \times 10^{-2}$	$1.6 \times 10^{-3}$
Froude number $Fr = U/\sqrt{g'H}/f$	1	0.3–1.2	0.9–1.1	1	0.6–1.3	1
Entrainment rate $W_e/U$	$5 \times 10^{-4}$	$1 \times 10^{-3}$	$6 \times 10^{-3}$		$2 \times 10^{-4}$	$5\text{--}20 \times 10^{-4}$
Coriolis parameter $f$ (s <sup>-1</sup> )	$1.3 \times 10^{-4}$	$1 \times 10^{-4}$	$1.3 \times 10^{-4}$	$1.3 \times 10^{-4}$	$1.3 \times 10^{-5}$	$3.1 \times 10^{-5}$
Deformation radius (km) $L_r = \sqrt{g'H}/f$	30	5	7	7	40	100

bode well for parameterization of gravity currents in the global ocean models.

Several different models are used by the team members (refer to Table 2 for model names). Each model's primary purpose is high-resolution nonhydrostatic simulation, regional or idealized calculations, global climate simulations, or a combination of the three. The global ocean models are all being used as the ocean component of coupled climate models. Simulation of overflows is especially sensitive to the vertical coordinate scheme, and the CPT has used each of the three principal types employed by ocean models today, so that we can find solutions that are most appropriate to each model type. Our strategy is to use process models to develop parameterizations and then to test and refine these parameterizations in the setting of an ocean general circulation model (OGCM), continuously referencing back to observations. Finally, the influence of the parameterization on coupled climate simulations can be evaluated.

Overflow process simulations have been conducted in idealized domains, including an overflow scenario developed as part of the earlier Dynamics

of Overflow Mixing and Entrainment (DOME) collaboration (Anderson 2004; Ezer and Mellor 2004; Ezer 2005). These have served to demonstrate the important physical processes operating in overflows and the sensitivity of simulated overflow mixing to both external parameters and model parameters, such as resolution, vertical coordinate, and subgrid-scale parameterizations. High-resolution idealized calculations also serve as benchmarks against which to test parameterizations in coarse-resolution simulations. Some of the process studies carried out as part of the CPT are documented in Ezer (2006), Legg et al. (2006, 2008), Özgökmen et al. (2004b,a, 2006), and Özgökmen and Fischer (2008).

### PHYSICAL PROCESSES IN OVERFLOWS.

Overflows include several different physical processes, all occurring below the resolution of most climate models. First, the dense water must often flow through a narrow channel or over a sill, where hydraulic processes may control the transport and mixing (Girton et al. 2006). Next, the dense water descends the continental slope, accelerating because of its density anomaly—often with augmentation

**TABLE 2. The different ocean models that have participated in the CPT. For details of the model configurations and parameterizations used, refer to the references listed. The model acronyms are defined as follows: Princeton Ocean Model generalized coordinate system (POMgcs) and Modular Ocean Model version 4 (MOM4). The parameterization acronyms include Mellor and Yamada (M–Y). Four of the ocean models listed form the ocean components of coupled modeling systems: MOM4 is the ocean component of climate model versions 2.1 (CM2.1) and 2M (CM2M); GOLD is the ocean component of CM2G; the CCSM ocean model is the ocean component of CCSM; and HYCOM is employed as an ocean component in CCSM and the NASA–GISS coupled model.**

Model	Vertical coordinate	Type of simulation	Gravity current parameterization/representation	CPT references
HYCOM	Hybrid/isopycnal/pressure	Process, regional, large scale	TPX MSBC	Chang et al. (2005, 2008) Xu et al. (2006, 2007)
MITgcm	pressure	Process, regional	Resolved; numerical diffusion	Legg et al. (2006, 2008) Riemenschneider and Legg (2007)
POMgcs	Terrain-following/generalized	Process	M–Y	Ezer and Mellor (2004) Mellor and Yamada (1982) Ezer (2005, 2006)
MOM4	pressure	Global	Campin–Goose cross-land diffusion Beckmann–Döscher	Griffies et al. (2005) Gnanadesikan et al. (2006)
CCSM	pressure	Global	MSBC	Wu et al. (2007) Yeager et al. (2006)
HIM/ GOLD	isopycnal	Process, global	JHS HBBL	Legg et al. (2006, 2008)
Nek5000	Finite element mesh	Process	Resolved	Özgökmen et al. (2004a,b; 2006; and 2008)

by thermobaric processes, especially in cold overflows (Gordon et al. 2004). Frictional processes at the seabed influence the flow field and mixing (Peters et al. 2005). The velocity difference between the accelerating dense water and the overlying water leads to shear instability at the upper interface of the overflow, resulting in entrainment of overlying water (Ellison and Turner 1959), diluting the overflow and increasing its transport (see Table 1). Some overflow fluid may detrain from the downslope current as it mixes with ambient water (Baines 2005). Planetary rotation may steer dense water along topographic contours. This geostrophic constraint must be broken, either in the Ekman layer or through baroclinic instability (Cenedese et al. 2004), to move dense water downslope. Eventually, the dense fluid may find a neutral buoyancy level and spread into the ocean interior, assisted by eddies resulting from baroclinic instability (Legg et al. 2006). If an ocean model is to produce deep or intermediate water at the correct rate, and location and tracer properties, it must account for the net result of these processes (Fig. 2). Different model types have to deal with different issues when modeling overflows. For example, height-coordinate models at very coarse resolutions have difficulty moving fluid down the slope without introducing excessive spurious mixing (Winton et al. 1998), whereas isopycnal models need to explicitly parameterize mixing or no entrainment will occur. All coarse-resolution models must determine how to deal with the subgrid-scale processes and topography that govern overflows.

The CPT framework has fostered two contrasting approaches that have been explored simultaneously. The first approach, known as the marginal sea boundary condition (MSBC; Price and Yang, 1998), removes overflow regions from the OGCM and uses inflow/outflow side boundary conditions to represent the net effects of the overflow, both upstream and downstream. These boundary conditions are the outputs of an overflow parameterization, which attempts to represent the important small-scale physical processes described above. In general, the inputs are the evolving ocean state (temperature, salinity, and density), both upstream and downstream of the overflow, as in the Community Climate System Model's (CCSM) Mediterranean overflow implementation

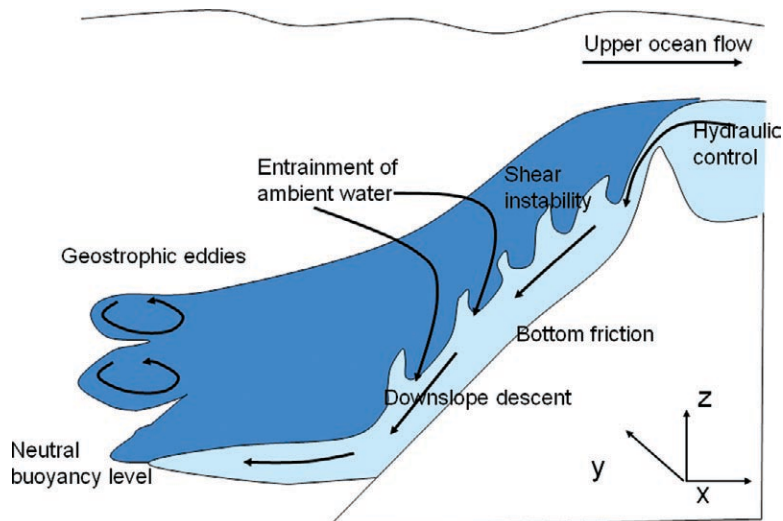


**FIG. 2.** Physical processes acting in overflows.

(Wu et al. 2007). The MSBC implementation in the Hybrid Coordinate Ocean Model (HYCOM), which does not have a prognostic representation of the Mediterranean, instead diagnoses the Mediterranean water properties from the climatological fluxes over the Mediterranean Basin.

The second approach attempts to parameterize the important overflow physics in terms of the OGCM's resolved current and density structure. Here, to illustrate the workings of the CPT and to show how results are being incorporated into climate models, we will focus on one process: the entrainment resulting from shear-driven mixing.

Prior to the start of the CPT, there were two parameterizations of shear-driven mixing commonly used in ocean climate models. In the first category, the Turner–Ellison parameterization (TE), has been implemented in isopycnal and hybrid-coordinate models [e.g. Generalized Ocean Layer Dynamics (GOLD), Miami Isopycnal Coordinate Ocean Model (MICOM), and HYCOM]. TE is derived from the bulk entrainment parameterization of Turner (1986) and Ellison and Turner (1959) and assumes that the net entrainment is proportional to the velocity shear times a function of the shear Richardson number ( $Ri$ ; Hallberg 2000), provided that  $Ri$  is less than some critical value. TE gives qualitatively reasonable depictions of gravity current entrainment in some circumstances (Papadakis et al. 2003; Legg et al. 2006) but leads to excessive shear-driven entrainment in the Pacific Equatorial Undercurrent when applied globally.

In the second category of parameterization, which includes the Pacanowski and Philander (1981) parameterization and the component of the  $K$ -profile

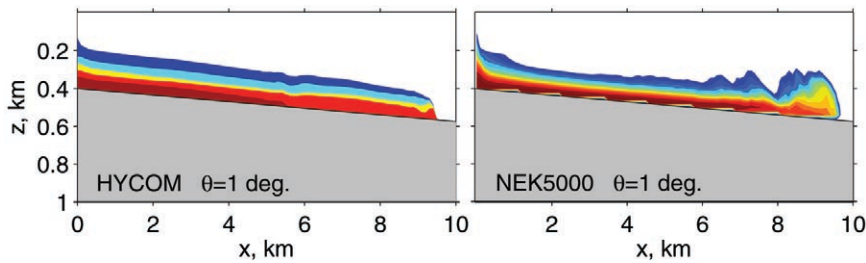


**Fig. 3. Snapshots showing vertical sections from 3D idealized bottom-gravity current experiments over smooth topography with a slope of  $\theta = 1^\circ$  from (left) HYCOM using the TPX parameterization, with a horizontal resolution of  $\Delta x = 100$  m and six isopycnal layers; and from (right) Nek5000 nonhydrostatic simulations, with a horizontal resolution of  $\Delta x = 33$  m and a vertical resolution of  $4 \text{ m} < \Delta z < 10 \text{ m}$ , about 3.25 h after the beginning of the calculation. The salinity anomaly is shown on a scale of 0–1 psu (anomalies of less than 0.2 psu appear white). Similar results were found for other bottom slopes. The Nek5000 simulations have been compared favorably with existing laboratory data in Özgökmen et al. (2004a). With the TPX parameterization, HYCOM is able to reproduce the coarse-grained structure of the nonhydrostatic results.**

parameterization (KPP; Large et al. 1994) applied in the stratified ocean interior, the shear-driven diffusivity is equal to a dimensional constant multiplied by a nondimensional function of shear  $Ri$ . These parameterizations were originally developed and calibrated for the shear-driven mixing in the equatorial Pacific, and there is a priori no reason to assume that they would be appropriate for overflows.<sup>1</sup>

A first step undertaken by the CPT was to evaluate TE and KPP, both implemented in HYCOM using idealized simulations of overflows, comparing and calibrating against 3D nonhydrostatic large-eddy simulations (LESs) from Özgökmen et al. [2004; using the parallel spectral element nonhydrostatic (Nek5000) model]. Whereas TE could be tuned to give good results compared to the LES, KPP has a preset upper limit to the diffusivity and therefore gives a less physical response (Chang et al. 2005). The best approximation using the same formalism as TE, found from a comprehensive study employing several LES calculations, is a linear parameterization known as the extended Turner parameterization (TPX):  $E = w_E / \Delta U = 0.20(1 - Ri/0.25)$  for  $Ri < 0.25$  and  $E = 0$  for  $Ri > 0.25$  (Xu et al. 2006), where  $E$  is the entrainment coefficient,  $w_E$  is the entrainment velocity, and  $\Delta U$  is the horizontal velocity difference between overflow and ambient water. TPX has now been implemented in HYCOM. Figures 3

<sup>1</sup> Fer (2006) shows that the Pacanowski and Philander (1981) parameterization only matches data from Arctic overflows if the values of the dimensional constants involved are increased more than tenfold compared to their values in the equatorial Pacific.

and 4 show that HYCOM simulations with the new parameterization compare well with nonhydrostatic Nek5000 simulations of three-dimensional gravity currents.

In parallel with these developments, a new parameterization of mixing driven by frictional processes at the bottom boundary, the Hallberg Bottom Boundary Layer model (HBBL), has been developed, inspired by the observed structure of the Red Sea outflow plume (Peters et al. 2005). Two distinct and well-defined regions of vigorous turbulent mixing are observed:

a stratified and sheared interfacial layer, well captured by TE; and a nearly homogenous turbulent bottom boundary layer. When TE is the only mixing parameterization in use, near-bottom viscous suppression of the shear keeps the bottommost water well stratified, and a sub-Ekman-layer thick sheet of overflow water flows into the abyss undiluted. Legg et al. (2006) find that the plume structure obtained with nonhydrostatic simulations with a horizontal resolution of 500 m can be reproduced nicely by the Hallberg Isopycnal Model (HIM) at a horizontal resolution of 10 km, employing HBBL where a specified fraction (here 20%, a typical efficiency for mechanically driven diapycnal mixing) of the energy extracted by the model's bottom drag is used to homogenize the near-bottom density.

Another track in parameterization development has been motivated by the observation that when TE-like parameterizations, tuned for overflows, are implemented globally, excessive mixing results in the Pacific Equatorial Undercurrent, where shear-driven mixing is also an important process. Specifically, when TE was implemented in the Geophysical Fluid Dynamics Laboratory (GFDL) global isopycnal model, realistic results were only achieved when the entrainment coefficient was reduced in the equatorial region; however, in a global model, it is not desirable to have to tune a shear-mixing parameterization individually for each location where it is applied. A new parameterization scheme, the Jackson–Hallberg scheme (JHS; Jackson et al. 2007), overcomes this problem with a model for diffusivity that is dependent on the shear forcing and a length scale. This

length scale is a combination of the width of the low Ri region and the buoyancy length scale over which turbulence decays; hence, mixing is reduced in the strongly stratified equatorial Pacific, where the buoyancy length scale is small. JHS also allows for a vertical transport of turbulence, from regions with a low Ri to the surrounding areas over a buoyancy length scale, an important physical process missing from parameterizations based on the local Ri (Fig. 5). JHS has been implemented into GOLD; global simulations show that credible results are produced both in the Pacific Equatorial Undercurrent and in the North Atlantic overflows with no additional tuning.

In summary, the CPT collaboration has led to the development of new and improved parameterizations of shear-driven mixing in overflows, which have been implemented in global isopycnal models (e.g. GOLD and HYCOM). GOLD is now being used as an ocean component of the GFDL coupled model system, and HYCOM is being used as an ocean component by several different coupled modeling groups; neither would have been possible prior to these new parameterization developments.

**IMPROVED CLIMATE MODELS: A CASE STUDY OF THE MEDITERRANEAN OUTFLOW.** To demonstrate the multipronged approach we have taken to improving ocean climate

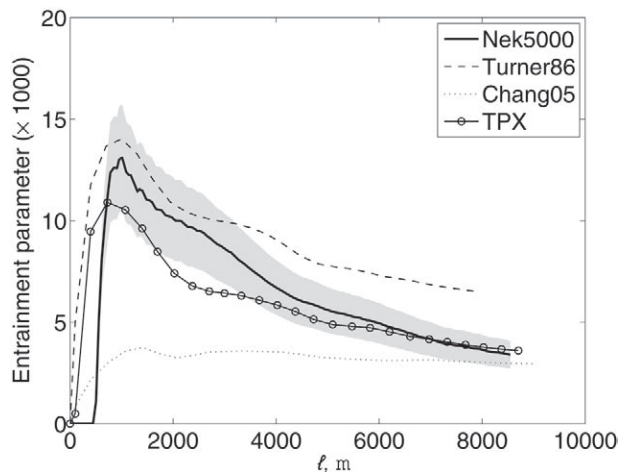


**FIG. 4. Comparison of the entrainment metric  $\varepsilon = (h - h_0)/l$ , the ratio of the difference between the average thickness ( $h$ ) and initial thicknesses ( $h_0$ ) of the plume, and the plume length ( $l$ ) from Nek5000 and HYCOM using different parameterizations of the entrainment  $E = W_s/\Delta U$ :  $E = (0.08 - 0.1\text{Ri})/(1 + 5\text{Ri})$  based on Turner (1986);  $E = 0.15(0.08 - 0.1\text{Ri})/(1 + 5\text{Ri})$  from Chang et al. (2005); and  $E = 0.2(1 - \text{Ri}/0.25)$ , the TPX parameterization, from Xu et al. (2006). The gray area represents the 20% “tolerance” band, where 20% has been chosen, since it is the range of variability shown by the Nek5000 simulations when the slope is varied by  $1^\circ$ . The new TPX parameterization falls within this band for most of the integration, unlike the older parameterizations from Turner (1986) and Chang et al. (2005).**

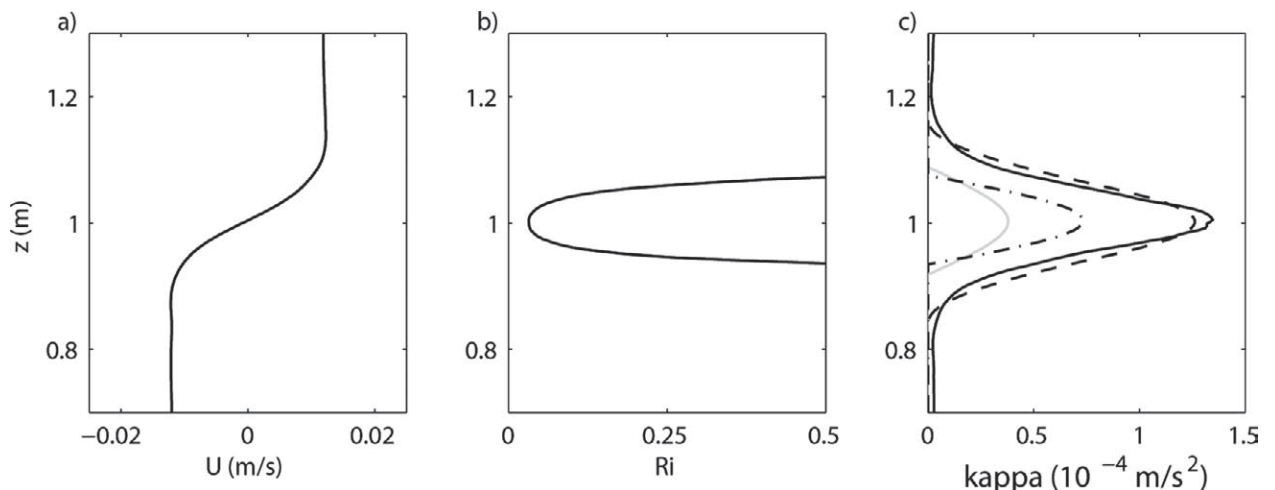


**FIG. 5. Comparison of parameterizations with high-resolution results for mixing in a stratified shear flow. (a) The velocity profile. (b) Ri (where only the region of low Ri is shown). (c) Eddy diffusivity diagnosed from a high-resolution 3D simulation of shear instability using the nonhydrostatic Massachusetts Institute of Technology (MIT) gcm (solid line); predicted eddy diffusivities from TE (gray line); TPX (dotted-dashed line); and JHS (dashed line). The horizontal mean shear flow shown in (a) and the stable background stratification are continually forced in the high-resolution simulation, so that the turbulent mixing is in a statistically steady state. The diffusivity profile shown in (c) was, for the high-resolution simulation, diagnosed from the temporal and horizontal averages of the explicitly simulated small-scale fluxes. For the parameterizations, the diffusivity profiles in (c) were calculated using the shear profile shown in (a) and the stable background stratification as inputs.**

model representation of overflows, we focus on the Mediterranean overflow. It is an attractive overflow for parameterization development and evaluation because the depth at which the overflow water equilibrates is highly sensitive to the amount of entrainment, and there are adequate field datasets that allow for detailed comparison with model results.

The Mediterranean overflow makes a dense, bottom-trapped gravity current that flows down the continental shelf and slope into the Gulf of Cadiz and then into the middepths of the eastern subtropical North Atlantic. At the Strait of Gibraltar (SOG), there is a two-layer baroclinic exchange flow with an outflow of saline Mediterranean water,  $S \approx 38.4$ , and an inflow of fresher North Atlantic water,  $S \approx 36.2$  (Price et al. 1993; Baringer and Price 1997). The volume transport in either layer has been reported in the range 0.7–1.0 Sv (Bryden et al. 1994; Candela 2001), and the salinity transport in the outflowing layer (salinity anomaly with respect to North Atlantic Central Water times volume transport) is 1.5–2.2 Sv.

As the Mediterranean overflow descends the continental shelf and slope of the Gulf of Cadiz, it

mixes intensely with the overlying North Atlantic water. Most of the mixing and resultant change in Mediterranean overflow salinity and temperature occurs within 100 km of the SOG, near the region where the overflow descends the shelf-slope break ( $6.1^\circ$ – $6.6^\circ$ W). In this 50-km segment of the path, the transport-weighted average of the salinity decreases from 38.0 to 36.5. An interesting feature of the Mediterranean overflow is the development of two distinct cores by about 100–150-km downstream, after the majority of the mixing has taken place. The deeper offshore core has a central density of about  $\sigma_\theta = 27.8 \text{ kg m}^{-3}$ , whereas the shallower onshore core has a density of  $\sigma_\theta = 27.5 \text{ kg m}^{-3}$ . This variation, not present within the SOG, results from differential entrainment (Baringer and Price 1997; Xu et al. 2007).

The properties of the Mediterranean overflow water (MOW) within the SOG (the source water) and the equilibrated, mixed Mediterranean water in the open North Atlantic (the product water) have been observed to change in the modern observational record. Whether these changes are a phase of a long period of oscillation or evidence of a secular drift is not clear. The densest MOW outflowing through the SOG has

warmed by  $0.15^\circ\text{C decade}^{-1}$  over the past several decades and has simultaneously become saltier by about  $0.03 \text{ decade}^{-1}$  (Millot et al. 2006). There has been little net change in density. The product water found in the open North Atlantic thermocline has also become warmer and saltier by roughly the same amount,  $0.1^\circ\text{C decade}^{-1}$  and  $0.03 \text{ decade}^{-1}$  (Potter and Lozier 2004).

Key features of the observations to be compared with numerical models are, therefore, the salinity and temperature difference and transport at the straits and downstream, the location and magnitude of entrainment, and the emergence of a double core structure. Whether and how changes in overflow product waters might result from changes in source waters is an important and relevant question for this CPT.

Regional simulation of the Mediterranean overflow, using HYCOM at high resolution with the TPX entrainment parameterization (Fig. 6), allows this parameterization to be evaluated by comparison with field

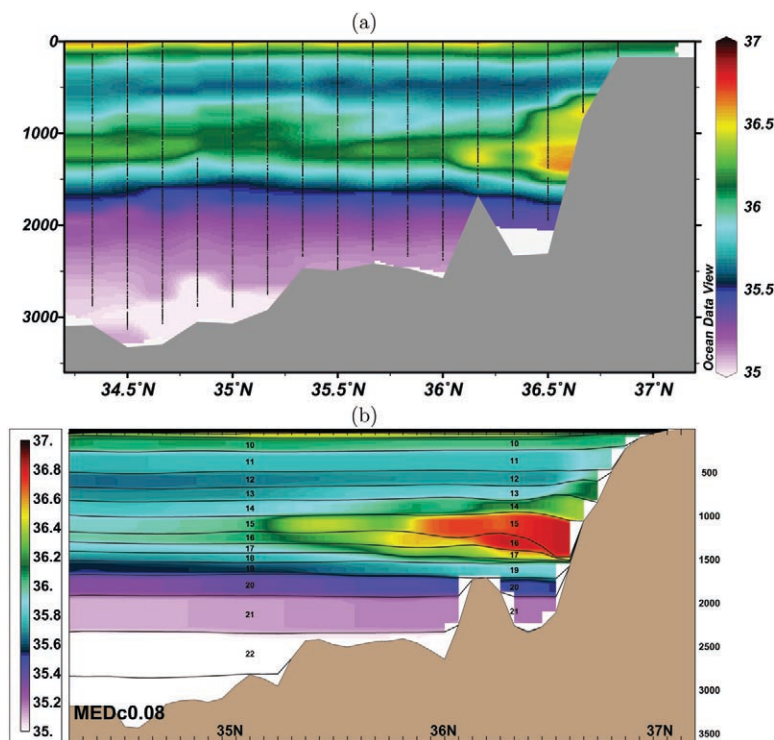


**FIG. 6.** Salinity in the Mediterranean outflow plume shown as a function of latitude and depth along a section at  $8.5^\circ$ W from (a) the World Ocean Circulation Experiment (WOCE) observations and (b) HYCOM regional simulation at  $0.08^\circ$  horizontal resolution with 28 layers in the vertical. The regional model was integrated for six months, and salinity is shown for the end of the integration.

data (Price et al. 1993).<sup>2</sup> The high-horizontal resolution allows for a reasonably realistic topography, and the regional HYCOM is able to reproduce quite well the major water property changes within about 150 km west of the SOG via entrainment as well as the transition of the outflow plume from a bottom-trapped gravity current to a wall-bounded undercurrent at about 8.5°W. The simulated MOW is, however, more saline and warmer than observed because of saltier ambient water (prescribed from climatology) and entrainment at a shallower location in the model, perhaps because the details of the topography near the sill are not resolved. However, the simulated MOW has the correct density and hence equilibrated depth. The simulated plume does not extend sufficiently far southward compared to observations because of the limited integration time (6 months).

The solution is sensitive to the choices made for horizontal and vertical resolution: coarser resolution results in less vigorous simulated currents (and associated vertical shear) and, consequently, less entrainment (Xu et al. 2007), which will influence coarse-resolution climate simulations with this same model.

As mentioned earlier, an alternative approach to explicitly simulating the outflow in a high-resolution model, as done above, is to use an outflow model, such as the Price and Yang (1998) MSBC. Because both the

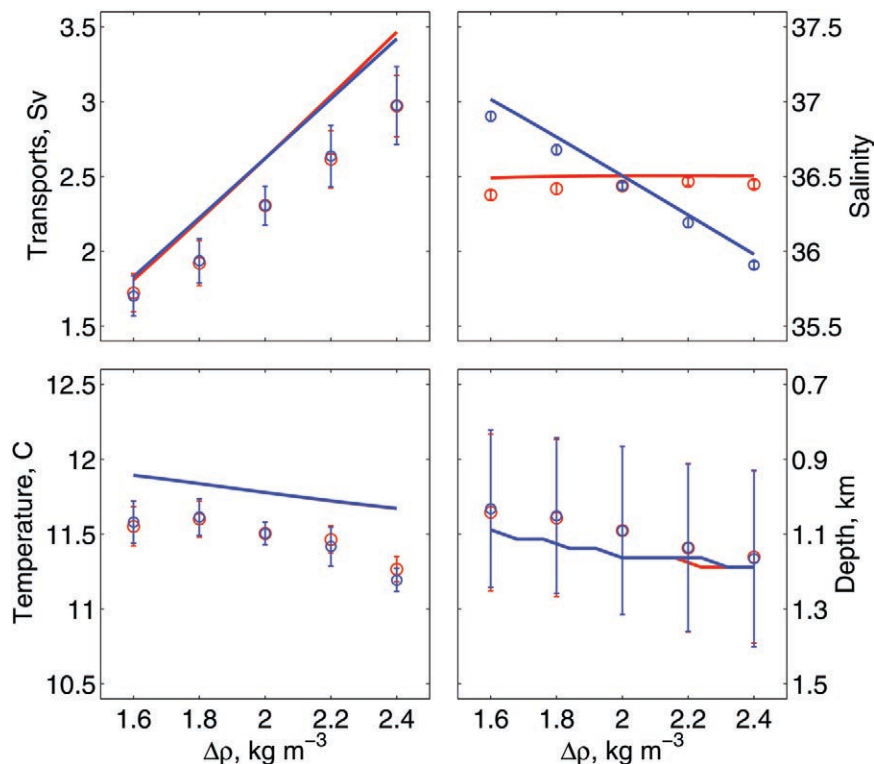


**FIG. 7.** The MOW product water properties as predicted by five HYCOM/TPX experiments (discrete circles) and by MSBC (lines). The abscissa is the density contrast between the Mediterranean Sea and the Gulf of Cádiz. The nominal (modern) value is  $2 \text{ kg m}^{-3}$ . The density contrast was changed by imposing an increase or decrease of salinity throughout the entire water column in either the Mediterranean Sea [red circles (HYCOM) and red lines (MSBC)] or in the Atlantic [blue circles (HYCOM) and blue lines (MSBC)]. The four panels are the resulting (upper left) overflow product water transport; (upper right) salinity; (lower left) temperature; and (lower right) equilibrium depth. The error bars (of HYCOM results) represent the standard deviation for transport, salinity, and temperature, and the mean upper and lower interface of outflow plume for depth. Generally, the trends of overflow properties are similar in the HYCOM and MSBC results. Unlike most other quantities, product water salinity does not change in a symmetric way with respect to changes in oceanic versus marginal sea properties, and this asymmetry in the salinity response shows up in a very similar way in both models.

regional simulations with HYCOM (Xu et al. 2007) and stand-alone calculations with MSBC (Price and Yang 1998) are able to reproduce the current state of the Mediterranean overflow reasonably well under present climate conditions, it is, therefore, useful to compare the sensitivity of MOW product water to changing conditions in both models. Our presumption is that the HYCOM/TPX regional model gives the more reliable result, since it is less idealized and constrained than the MSBC. Hence, if the MSBC in stand-alone form is found to agree with the HYCOM simulations, then it would appear to be a viable candidate for use in a coarse-resolution climate model that would not otherwise represent the Mediterranean outflow.

<sup>2</sup> TPX was used rather than JHS because the latter was developed later in the study and only recently implemented in a GCM. Idealized simulations (Legg et al. 2008) show that TPX and JHS perform very similarly in overflow regions.

To this end, two sets of experiments employing the regional HYCOM and the MSBC were designed to investigate the sensitivity of the outflow product water to imposed variations of the outflow source water and ambient oceanic water, which might result from variations in air–sea fluxes in the Mediterranean Basin and subtropic North Atlantic, respectively. As shown in Fig. 7, these two experiments give very similar predictions for the sensitivity of MOW product water in terms of volume transport, temperature and salinity properties, and equilibrium depth. An important result common to both models is that the salinity of the product waters is remarkably insensitive to density change in the outflow source water, and yet it is quite sensitive to a similar change in the oceanic water. Because of the dilution of MOW source water by entrainment, a (small) increase of the deep-water salinity in the Mediterranean Basin will be expected to result in a somewhat greater volume of MOW product water having only a very slightly increased salinity (Xu et al. 2007). Thus, the roughly similar increase in temperature and salinity observed in the climatology of source and product waters of the Mediterranean overflow may not be the cause and effect it first appears [refer to Potter and Lozier (2004) and Lozier and Stewart (2008)].

Having shown that the MSBC in stand-alone form is able to reproduce the results of an explicit regional simulation of the Mediterranean outflow under changing climate conditions, we proceeded to implement this overflow representation into a fully coupled climate model. We implemented a modified version of the MSBC [referred to as the parameterized Mediterranean outflow (PMO)] in the ocean component of the National Center for Atmospheric Research (NCAR) Community Climate System Model, version 3 (CCSM3), using the table of observations to guide the choice of specified parameters. This modified MSBC allows for an evolving, resolved Mediterranean Basin, where the original MSBC presumed a box model. In coupled simulations, the challenge is to obtain a stable, realistic solution over hundreds of years. So that long integrations would be feasible, we used the low (nominally 3°)-resolution ( $T31 \times 3$ ) version of CCSM3 (Yeager et al. 2006). Detailed comparisons of solutions after 300 yr from control simulations with a blocked SOG and from experiments with the PMO for ocean-only and coupled cases are presented in Wu et al. (2007) and briefly summarized next.

After spinup, the volume transports of the source water with PMO are 0.74 and 0.84 Sv in ocean-only and coupled simulations, respectively. The volume of entrained North Atlantic water is 0.96 and 1.03 Sv

in ocean-only and coupled simulations, respectively. Both the source and entrained water transports remain at the lower limits of observational estimates (shown in Table 1). Similarly, the product water transports fall below the observational range to 1.70 (ocean only) and 1.87 Sv (coupled), but to obtain such reasonable results at low resolution is encouraging.

Figures 8a and 8b compare the PMO and control results for year 30 of the ocean-only simulations. The Mediterranean salt tongue is completely missing in the control integration, but it is clearly present in the PMO simulation. In comparison with the observations (Fig. 8f), the PMO tends to produce a saltier and warmer salt tongue. As detailed in Wu et al. (2007), the influence of MOW on the Atlantic MOC is relatively small and with PMO, the MOC has a 15% decrease. Other studies (Rahmstorf 1998) report an increase in MOC when the MOW is included. The Mediterranean overflow, while a good test bed for parameterizations, it is not the most important overflow to climate. Instead, we expect the MOC to be much more sensitive to the Nordic overflows, investigation of which is currently in progress.

A parallel track to the implementation of the MSBC in the CCSM has been the implementation of new developments in GOLD. Prior to the CPT, this model used the TE shear-driven mixing parameterization. As in most coarse-resolution models, the SOG was set to the size of the model grid, 111 km, much wider than the actual straits. In this configuration there was an overly strong exchange through SOG, roughly 5 Sv averaged over the first year, that leads to a strong salty drift in the MOW and a fresh drift in the Mediterranean (Fig. 8c). Restricting the width of SOG to its true width of 12 km, using a new algorithm for “partially open barriers,” which allows for channels of subgrid-scale width, immediately reduces the transport through the channel to realistic levels.<sup>3</sup> Despite these improvements, with just the TE parameterization, the MOW develops two plumes: one plume that exhibits reasonable levels of entrainment and a second plume of nearly undiluted overflow water within the bottom Ekman layer (Fig. 8d). This separated deeper plume is eliminated by using the HBBL parameterization (Fig. 8e), and now the overflow plume has a salinity, density, and

<sup>3</sup> As currently implemented in GOLD, the partially open barriers only apply to full-depth channels, such as Gibraltar or Bab-el-Mandeb; however, there is work underway to make the open width a function of depth, making them equally beneficial for submerged barriers like those around the Faroe Bank Channel or Romanche Fracture Zone.

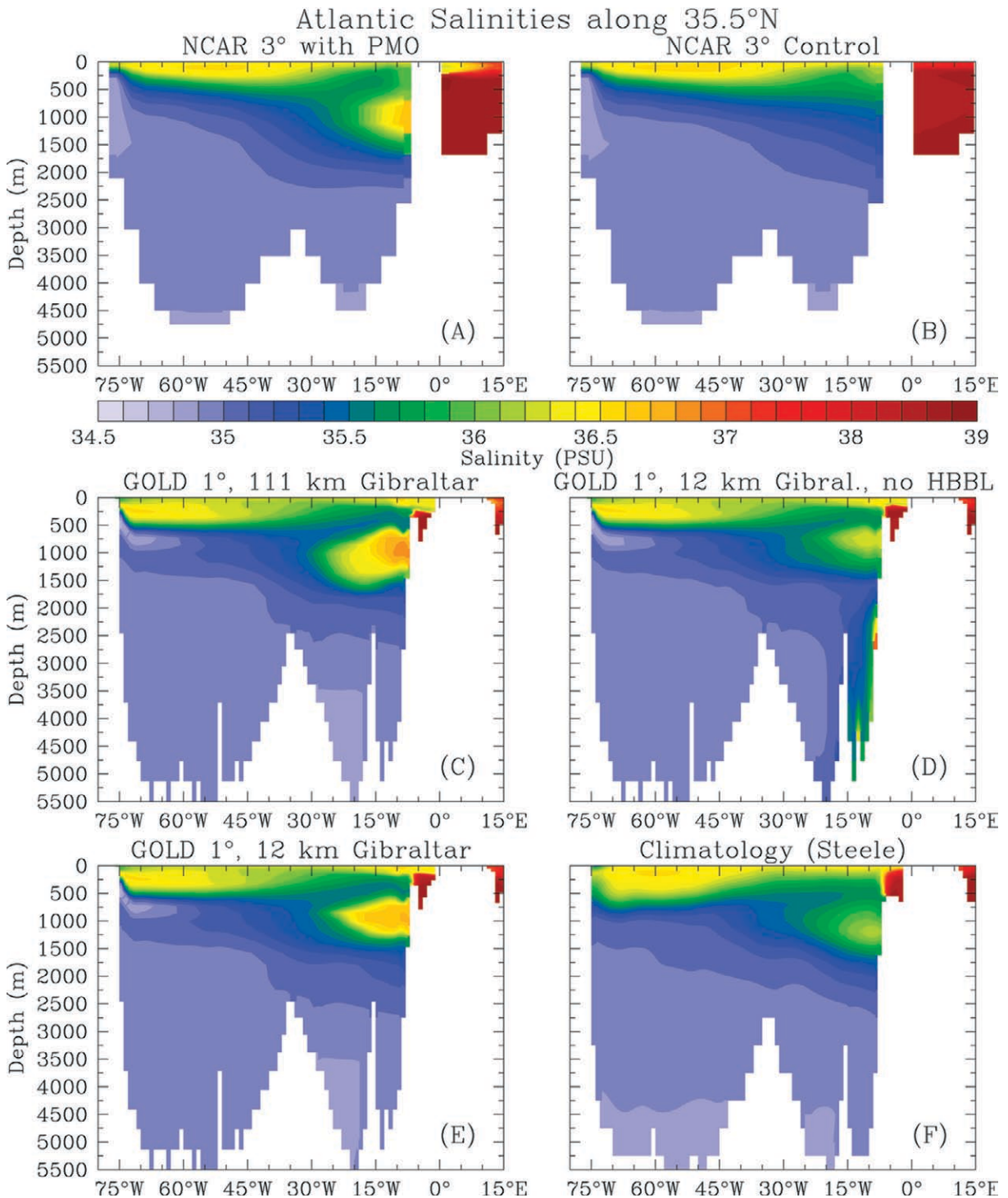


**FIG. 8.** Salinity cross sections in the Atlantic Ocean at the latitude of the SOG. (top) Comparing the results after 30 yr with the (left) NCAR ocean-only simulations with the PMO and (right) a control experiment in which the SOG is blocked. These simulations use the nominal 3° resolution version of the model. The improvements due to the PMO are obvious. The results after 10 years in GFDL’s 1° isopycnal coordinate, GOLD, with (c) Gibraltar open at 111 km (1 grid point) width; (d) Gibraltar restricted to 12 km but without the HBBL parameterization; and (e) both TE and HBBL parameterizations activated. (f) The salinity in the Steele ocean climatology; the data processing behind this climatology includes enough temporal and spatial smoothing that the “climatological” salinity of the plume is lower by several tenths of a psu compared with raw profiles, but it should be reflective of the depth and extent of the plume. The SOG itself is between 5° and 6°W and between 0° and 10°E this section goes through North Africa.

volume much closer to that seen in observations (Fig. 8f).

In summary, the CPT has led to improvements in the representation of the Mediterranean overflow, demonstrated here in two different global ocean models (CCSM and GOLD), which form the ocean components of coupled climate models.

**CONCLUDING REMARKS.** We have described here how the Gravity Current Entrainment Climate Process Team effort has led to new parameterizations of overflow processes and how the implementation of those parameterizations in the Mediterranean overflow has led to significant improvement in simulations carried out by the ocean components of climate models. Similar approaches have been taken to develop improvements for the Faroe Bank Channel and the Denmark Straits overflows and Red Sea overflow, where results from regional simulations carried out by CPT members (Riemenschneider and Legg 2007; Pratt et al. 2007; Chang et al. 2008) and other researchers (Käse et al. 2003) are being used to guide the implementation of parameterizations in OGCMs. Early results from coupled simulations at both NCAR and GFDL indicate a significant influence of the improved Nordic overflow representation on North Atlantic sea surface temperatures. Finally, work is currently underway to translate these improvements to the Antarctic overflows.

An important goal of the CPT is to evaluate the influence of overflow processes on the climate. Earlier studies using  $z$ -coordinate ocean models in a coupled modeling system (Tang and Roberts 2005; Kösters et al. 2005; Lohmann 1998) have shown that including the downslope dense-water transport due to overflows leads to changes in the MOC and associated climate features but are not conclusive as to the role of overflows on the stability of the MOC.<sup>4</sup> Now as the new overflow entrainment parameterizations are implemented into coupled climate models, we are beginning to investigate the influence of overflow entrainment on the large-scale circulation and, therefore, climate. We are guided by work carried out in idealized ocean models, which suggest that overflow entrainment can significantly influence the MOC and large-scale ocean stratification (Hughes and Griffiths 2006; Wahlin and Cenedese 2006). Early results from the NCAR and GFDL OGCMs

<sup>4</sup> These earlier studies did not include physically based parameterizations of the entrainment in overflows but rather focused on limiting the excessive spurious entrainment in the  $z$ -coordinate models.

suggest that much of the North Atlantic is influenced by the overflows, with changes in the deep western boundary current leading to changes in the overlying Gulf Stream [as shown in earlier process studies, e.g., Zhang and Vallis (2007)] and, therefore, influencing air–sea heat transfer. Future work will examine the role overflows play in variations in the MOC, whether as a result of increased freshwater input or in past climate scenarios.

The successful development and implementation of parameterizations in the ocean components of several climate models by this CPT would not have been possible without the serious input and effort of observationalists and process modelers, combined with the involvement of multiple modeling teams. Workshops and special sessions at large conferences have played an important role in encouraging this dialogue. Importantly, several ideas for parameterization, for example, the MSBC and the TE parameterization, were already formulated before the start of the CPT, so that real progress was possible in implementing parameterizations into climate models in a relatively short time. The pursuit of several different avenues for parameterization has been important in ensuring diversity in approach and encouraging new solutions. This collaboration between model developers, process researchers, and field observationalists is one that has helped to ensure that our best present understanding of overflows has been incorporated into the development of OGCMs in a timely way.

**ACKNOWLEDGMENTS.** The Gravity Current Entrainment Climate Process Team was funded by NSF grants OCE-0336850 and OCE-0611572 and NOAA as a contribution to U.S.CLIVAR.

## REFERENCES

- Anderson, W., 2004: Oceanic sill-overflow systems: Investigation and simulation with the Poseidon ocean general circulation model. Ph.D. dissertation, George Mason University, 125 pp.
- Baines, P., 2005: Mixing regimes for the flow of dense fluid down slopes into stratified environments. *J. Fluid. Mech.*, **538**, 245–267.
- Baringer, M. O., and J. F. Price, 1997: Mixing and spreading of the Mediterranean outflow. *J. Phys. Oceanogr.*, **27**, 1654–1677.
- Bryden, H. L., J. C. Candela, and T. H. Kinder, 1994: Exchange through the Strait of Gibraltar. *Progr. Oceanogr.*, **33**, 201–248.
- Candela, J., 2001: Mediterranean water and global circulation. *Ocean Circulation and Climate*, G. Siedler,

- J. Church, and J. Gould, Eds., Academic Press, 419–429 pp.
- Cenedese, C., J. A. Whitehead, T. Ascarelli, and M. Ohiwa, 2004: A dense current flowing down a sloping bottom in a rotating fluid. *J. Phys. Oceanogr.*, **34**, 188–203.
- Chang, Y. S., X. Xu, T. Özgökmen, E. P. Chassignet, H. Peters, and P. F. Fischer, 2005: Comparison of gravity current mixing parameterizations and calibration using a high-resolution 3D nonhydrostatic spectral element model. *Ocean Modell.*, **10**, 342–368.
- , T. Özgökmen, H. Peters, and X. Xu, 2008: Numerical simulation of the Red Sea outflow using HYCOM and comparison with REDSOX observations. *J. Phys. Oceanogr.*, **38**, 337–358.
- Dickson, R. B., and J. Brown, 1994: The production of North Atlantic Deep water: Source, rates, and pathways. *J. Geophys. Res.*, **99**, 12 319–12 341.
- Ellison, T. H., and J. S. Turner, 1959: Turbulent entrainment in stratified flows. *J. Fluid Mech.*, **6**, 423–448.
- Ezer, T., 2005: Entrainment, diapycnal mixing and transport in three-dimensional bottom gravity current simulations using the Mellor-Yamada turbulence scheme. *Ocean Modell.*, **9**, 151–168.
- , 2006: Topographic influence on overflow dynamics: Idealized numerical simulations and the Faroe Bank Channel overflow. *J. Geophys. Res.*, **111**, C02002, doi:10.1029/2005JC003195.
- , and G. Mellor, 2004: A generalized coordinate ocean model and comparison of the bottom boundary layer dynamics in terrain-following and in  $z$ -level grids. *Ocean Modell.*, **6**, 379–403.
- Fer, I., 2006: Scaling turbulent dissipation in an arctic fjord. *Deep-Sea Res. II*, **53**, 77–95.
- Foldvick, A., and Coauthors, 2004: Ice shelf water overflow and bottom water formation in the southern Weddell Sea. *J. Geophys. Res.*, **109**, C02015, doi:10.1029/2003JC002008.
- Girton, J. B., and T. B. Sanford, 2003: Descent and modification of the overflow plume in the Denmark Strait. *J. Phys. Oceanogr.*, **33**, 1351–1363.
- , L. J. Pratt, D. Sutherland, and J. Price, 2006: Is the Faroe Bank Channel overflow hydraulically controlled? *J. Phys. Oceanogr.*, **36**, 2340–2349.
- Gnanadesikan, A., and Coauthors, 2006: GFDL's CM2 global coupled climate models. Part II: The baseline ocean simulation. *J. Climate*, **19**, 675–697.
- Gordon, A., E. Zambianchi, A. Orsi, M. Visbeck, C. Giulivi, T. Whitworth III, and G. Spezie, 2004: Energetic plumes over the western Ross Sea continental slope. *Geophys. Res. Lett.*, **31**, L21302, doi:10.1029/2004GL020785.
- Griffies, S. M., and Coauthors, 2005: Formulation of an ocean model for global climate simulations. *Ocean Sci.*, **1**, 45–79.
- Hallberg, R., 2000: Time integration of diapycnal diffusion and Richardson number-dependent mixing in isopycnal coordinate ocean models. *Mon. Wea. Rev.*, **128**, 1402–1419.
- Hughes, G., and R. Griffiths, 2006: A simple convective model of the overturning circulation, including effects of entrainment into sinking regions. *Ocean Modell.*, **12**, 46–79.
- Jackson, L., R. Hallberg, and S. Legg, 2008: A parameterization of shear-driven turbulence for ocean climate models. *J. Phys. Oceanogr.*, **38**, 1033–1053.
- Käse, R. H., J. B. Girton, and T. B. Sanford, 2003: Structure and variability of the Denmark Strait Overflow: Model and observations. *J. Geophys. Res.*, **108** (C6), 3181, doi:10.1029/2002JC001548.
- Kida, S., J. Price, and J. Yang, 2008: The upper-oceanic response to overflows: A mechanism for the Azores Current. *J. Phys. Oceanogr.*, **38**, 880–895.
- Kösters, F., R. H. Käse, A. Schmittner, and P. Herrmann, 2005: The effect of Denmark Strait overflow on the Atlantic Meridional Overturning Circulation. *Geophys. Res. Lett.*, **32**, L04602, doi:10.1029/2004GL022112.
- Large, W. G., J. C. McWilliams, and S. C. Doney, 1994: Ocean vertical mixing: A review and a model with a nonlocal boundary layer parameterization. *Rev. Geophys.*, **32**, 363–403.
- Legg, S., R. Hallberg, and J. Girton, 2006: Comparison of entrainment in overflows simulated by  $z$ -coordinate, isopycnal and nonhydrostatic models. *Ocean Modell.*, **11**, 69–97.
- , L. Jackson, and R. Hallberg, 2008: Eddy-resolving modeling of overflows. *Eddy-Resolving Ocean Modeling*, *Geophys. Monogr.*, Vol. 17, Amer. Geophys. Union, 63–82.
- Lohmann, G., 1998: The influence of a near-bottom transport parameterization on the sensitivity of the thermohaline circulation. *J. Phys. Oceanogr.*, **28**, 2095–2103.
- Lozier, M., and N. Stewart, 2008: On the temporally varying northward penetration of Mediterranean Overflow Water and eastward penetration of Labrador Sea water. *J. Phys. Oceanogr.*, **38**, 2097–2103.
- Mauritzen, C., J. Price, T. Sanford, and D. Torres, 2005: Circulation and mixing in the Faroese Channels. *Deep-Sea Res. I*, **52**, 883–913.
- Mellor, G. L., and T. Yamada, 1982: Development of a turbulence closure model for geophysical fluid problems. *Rev. Geophys.*, **20**, 851–875.

- Millot, C., J. Candela, J. L. Fuda, and Y. Tber, 2006: Large warming and salinification of the Mediterranean outflow due to changes in its composition. *Deep-Sea Res. I*, **53**, 423–442.
- Özgökmen, T. M., and P. Fischer, 2008: On the role of bottom roughness in overflows. *Ocean Modell.*, **20**, 336–361.
- , —, J. Duan, and T. Iliescu, 2004a: Entrainment in bottom gravity currents over complex topography from three-dimensional nonhydrostatic simulations. *Geophys. Res. Lett.*, **31**, L13212, doi:10.1029/2004GL020186.
- , —, —, and —, 2004b: Three-dimensional turbulent bottom density currents from a high-order nonhydrostatic spectral element model. *J. Phys. Oceanogr.*, **34**, 2006–2026.
- , —, and W. E. Johns, 2006: Product water mass formation by turbulent density currents from a high-order nonhydrostatic spectral element model. *Ocean Modell.*, **12**, 237–267.
- Pacanowski, R. C., and S. G. H. Philander, 1981: Parameterization of vertical mixing in numerical models of the tropical oceans. *J. Phys. Oceanogr.*, **11**, 1443–1451.
- Papadakis, M. P., E. P. Chassignet, and R. W. Hallberg, 2003: Numerical simulations of the Mediterranean Sea outflow: Impact of the entrainment parameterization in an isopycnic coordinate model. *Ocean Modell.*, **5**, 325–356.
- Peters, H., W. E. Johns, A. S. Bower, and D. M. Fratantoni, 2005: Mixing and entrainment in the Red Sea outflow plume. Part I: Plume structure. *J. Phys. Oceanogr.*, **35**, 569–583.
- Potter, R. A., and M. S. Lozier, 2004: On the warming and salinification of the Mediterranean outflow in the North Atlantic. *Geophys. Res. Lett.*, **31**, L01202, doi:10.1029/2003GL018161.
- Pratt, L., U. Riemenschneider, and K. Helfrich, 2007: A transverse hydraulic jump in a model of the Faroe Bank Channel outflow. *Ocean Modell.*, **19**, 1–9.
- Price, J. F., and J. Yang, 1998: Marginal sea overflows for climate simulations. *Ocean Modelling and Parameterization*, E. Chassignet and J. Vernon, Eds., Kluwer Academic, 155–170.
- , and Coauthors, 1993: Mediterranean outflows and dynamics. *Science*, **259**, 1277–1282.
- Rahmstorf, S., 1998: Influence of Mediterranean outflow on climate. *Eos, Trans. Amer. Geophys. Union*, **79**, 281–282.
- Riemenschneider, U., and S. Legg, 2007: Regional simulations of the Faroe Bank Channel overflow in a level model. *Ocean Modell.*, **17**, 93–122.
- Solomon, S. D., D. Quin, M. Manning, M. Marquis, K. Averyt, M. M. B. Tignor, H. L. Miller Jr., and Z. Chen, Eds., 2007: *Climate Change 2007: The Physical Sciences Basis*. Cambridge University Press, 996 pp.
- Stouffer, R., and Coauthors, 2006: Investigating the causes of the response of the thermohaline circulation to past and future climate changes. *J. Climate*, **19**, 1365–1387.
- Tang, Y. M., and M. J. Roberts, 2005: The impact of a bottom boundary layer scheme on the North Atlantic Ocean in a global coupled climate model. *J. Phys. Oceanogr.*, **35**, 202–217.
- Turner, J. S., 1986: The development of the entrainment assumption and its application to geophysical flows. *J. Fluid Mech.*, **173**, 431–471.
- Wahlin, A., and C. Cenedese, 2006: How entraining density currents influence the stratification in a one-dimensional ocean basin. *Deep Sea Res. II*, **53**, 172–193.
- Winton, M., R. Hallberg, and A. Gnanadesikan, 1998: Simulation of density-driven frictional downslope flow in z-coordinate ocean models. *J. Phys. Oceanogr.*, **28**, 2163–2174.
- Wu, W., G. Danabasoglu, and W. Large, 2007: On the effects of parameterized Mediterranean overflow on North Atlantic ocean circulation and climate. *Ocean Modell.*, **19**, 31–52, doi:10.10106/j.ocemod.2007.06.003.
- Xu, X., Y. S. Chang, H. Peters, T. M. Özgökmen, and E. P. Chassignet, 2006: Parameterization of gravity current entrainment for ocean circulation models using a high-order 3D nonhydrostatic spectral element model. *Ocean Modell.*, **14**, 19–44.
- , E. P. Chassignet, J. F. Price, T. M. Özgökmen, and H. Peters, 2007: A regional modeling study of the entraining Mediterranean outflow. *J. Geophys. Res.*, **112**, C12005, doi:10.1029/2007JC004145.
- Yang, J., and J. Price, 2007: Potential vorticity constraint on the flow between two basins. *J. Phys. Oceanogr.*, **37**, 2251–2266.
- Yeager, S., C. Shields, W. Large, and J. Hack, 2006: The low-resolution CCSM3. *J. Climate*, **19**, 2545–2566.
- Zhang, R., and G. Vallis, 2007: The role of bottom vortex stretching on the path of the North Atlantic western boundary current and on the northern recirculation gyre. *J. Phys. Oceanogr.*, **37**, 2053–2080.